Supporting Information

Nanopolyhedral Zn/Fe-NC derived from bimetallic zeolitic imidazole frameworks as an efficient catalyst for oxygen reduction reaction in an air-cathode microbial fuel cell

Qianwu Wang[abc], Jingzhao Lu[d], Songlin Liu[c], Boqu Yu[ae], Bolong Liang[a*]

a. School of Eco-Environment, Hebei Key Laboratory of Close-to-Nature Restoration Technology of Wetlands, Hebei University, Baoding 071002, China

b. Beijing Construction Engineering Group Environmental Remediation Co., Ltd.

c. College of Environmental Science and Engineering, Nankai University, Tianjin 300350, China

d. College of Science and Technology, Hebei Agricultural University, Cangzhou 061100, China

e. State Key Laboratory of Pollution Control and Resource Reuse, Nanjing University, Nanjing 210093, China

[*] Corresponding author. E-mail: liangbolong@hbu.edu.cn

Text S1

The components of PBS solution

The PBS consists of NH_4Cl (0.31 g L^{-1}), KCl (0.13 g L^{-1}), $NaH_2PO_4 \cdot 2H_2O$ (3.321 g L^{-1}), Na_2HPO_4 (4.090 g L^{-1}), trace mineral (12.5 mL L^{-1}), and vitamin (5 mL L^{-1}) solution.

Table S1

Porous structure parameters of different cathodes.

Samples	NC	Zn/Fe-NC-0.1	Zn/Fe-NC-0.3	Zn/Fe-NC-0.5	Zn/Fe-NC-0.7	Zn/Fe-NC-0.9
BET Surface Area (m^2/g)	1371.59	1049.70	982.60	1023.01	1120.62	805.17
Micropore Area (m^2/g)	1160.11	938.6	874.16	941.83	988.35	727.41
Mesopore Area (m^2/g)	211.48	111.10	108.44	81.18	132.27	77.76
Total pore volume (cm^3/g)	0.674	0.483	0.467	0.454	0.526	0.360
Micropore volume (cm^3/g)	0.583	0.427	0.407	0.412	0.461	0.317
Average Pore Size (nm)	1.96	1.84	1.90	1.78	1.88	1.78

Table S2

Element contents of all samples measured from XPS analysis (at. %).

Samples	Total N	N type			
		Pyridinic N	Pyrrolic N or Fe-N	Graphitic N	Oxidized N
NC	7.31	47	15	26	12
Zn/Fe-NC-0.1	6.81	43	20	22	15
Zn/Fe-NC-0.3	7.12	44	19	23	14
Zn/Fe-NC-0.5	7.46	45	20	25	10
Zn/Fe-NC-0.7	7.43	44	20	24	12
Zn/Fe-NC-0.9	7.20	43	24	22	11

Table S3

Fe 2p of all samples measured from XPS analysis (at. %).

Samples	Fe 2p			
	2p3/2 Fe^{3+}	2p3/2 Fe^{2+}	2p1/2 Fe^{2+}	Fe-C bond
Zn/Fe-NC-0.1	30.89	26.68	33.45	8.98
Zn/Fe-NC-0.3	25.49	37.89	26.69	9.93
Zn/Fe-NC-0.5	29.90	32.27	26.21	11.62
Zn/Fe-NC-0.7	26.78	35.51	32.74	4.97
Zn/Fe-NC-0.9	19.88	43.17	32.75	4.20

Table S4

The onset potential and half-wave potential for ORR for the catalysts

Samples	Onset potential (vs. Ag/AgCl)	Onset potential (vs. SHE)	Half-wave potential (vs. Ag/AgCl)	Half-wave potential (vs. SHE)
Zn/Fe-NC-0.1	0.158 V	0.353 V	-0.017 V	0.178 V
Zn/Fe-NC-0.3	0.169 V	0.364 V	-0.002 V	0.193 V
Zn/Fe-NC-0.5	0.236 V	0.431 V	0.053 V	0.248 V
Zn/Fe-NC-0.7	0.205 V	0.400 V	0.051 V	0.246 V
Zn/Fe-NC-0.9	0.162 V	0.357 V	-0.008 V	0.187 V
10% Pt/C	0.195 V	0.390 V	0.005 V	0.200 V

Table S5

Compare the performance of MFCs with different cathode catalysts.

Catalyst	Anode	Cathode	Device type	Max. p (mW m^{-2})	Ref.
Fe-N-C	Carbon fiber brush	Carbon cloth	Single chamber	1308	[1]
Fe-N/C	Carbon fiber brush	Carbon paper	Single chamber	1232.9	[2]
Fe-N_x/C	Carbon fiber brush	Carbon cloth	Single chamber	1227	[3]
Fe/N-HCN	Graphite fiber brush	Carbon cloth	Single chamber	1300	[4]
Fe-N-C/G	Graphite felt	Carbon fiber cloth	Single chamber	1601	[5]
Cu@N-C	Carbon felt	Stainless-steel mesh	Single chamber	1760	[6]
Zn/Fe-NC-0.5	Carbon felt	Stainless-steel mesh	Single chamber	1954	This work

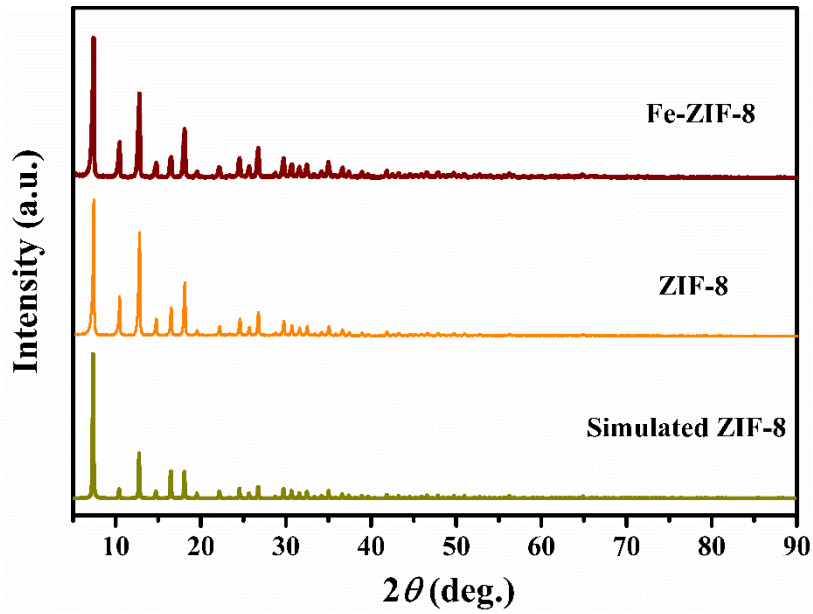

Fig. S1. XRD patterns of ZIF-8 and Fe-ZIF-8. (Note that Fe-ZIF-8 is the sample, which is the 0.5g of $Fe(acac)_3$ added)

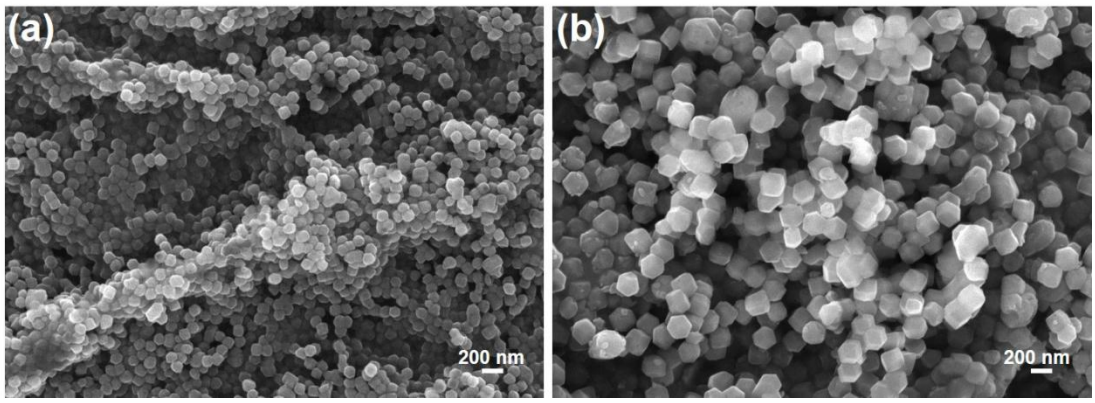

Fig. S2. SEM images of (a) ZIF-8 and (b) Fe-ZIF-8. (Note that Fe-ZIF-8 material is the sample, which is the 0.5g of $Fe(acac)_3$ added)

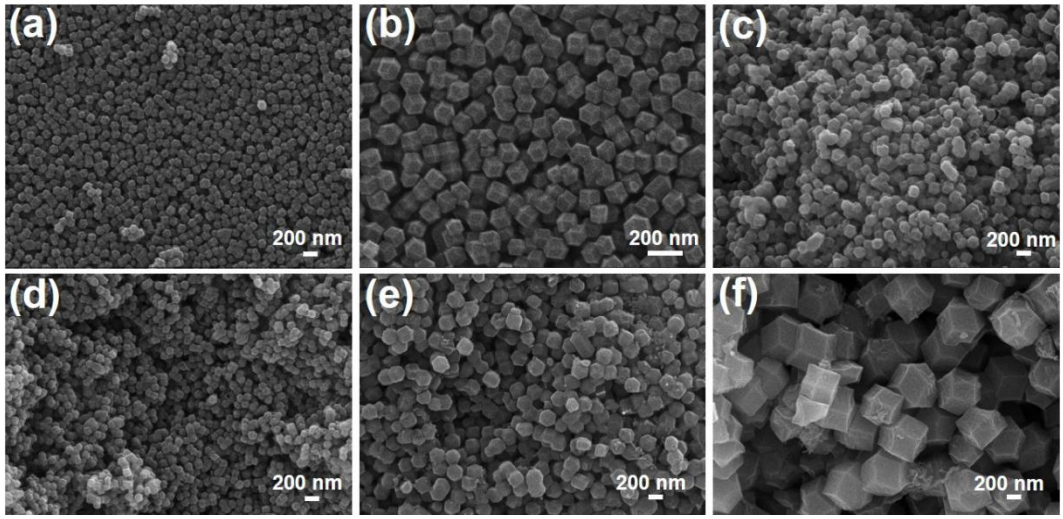

Fig. S3. SEM images of (a-b) NC, (c) Zn/Fe-NC-0.1, (d) Zn/Fe-NC-0.3, (e) Zn/Fe-NC-0.7 and (f) Zn/Fe-NC-0.9.

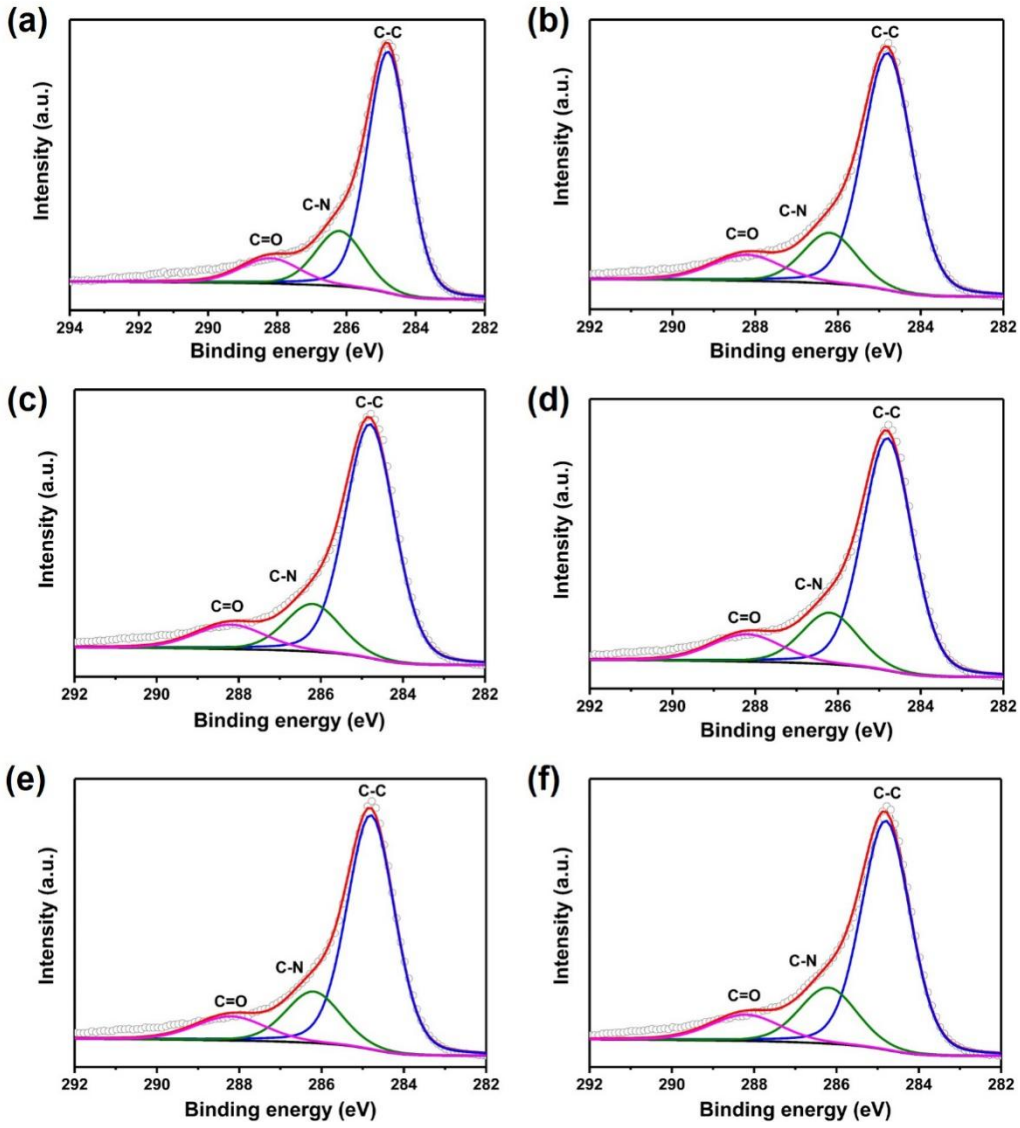

Fig. S4. C 1s XPS spectra of (a) NC, (b) Zn/Fe-NC-0.1, (c) Zn/Fe-NC-0.3, (d) Zn/Fe-NC-0.5, (e) Zn/Fe-NC-0.7 and (f) Zn/Fe-NC-0.9.

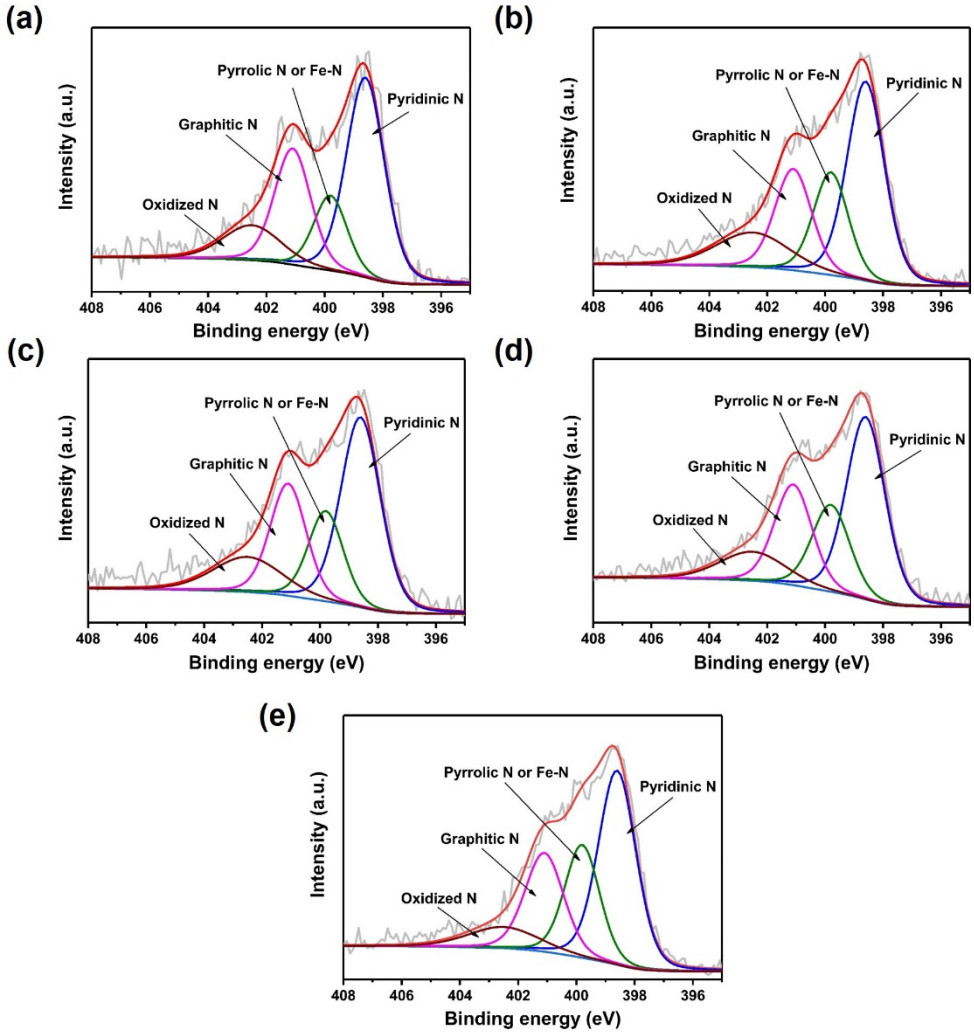

Fig. S5. N 1s XPS spectra of (a) NC, (b) Zn/Fe-NC-0.1, (c) Zn/Fe-NC-0.3, (d) Zn/Fe-NC-0.7, (e) Zn/Fe-NC-0.9

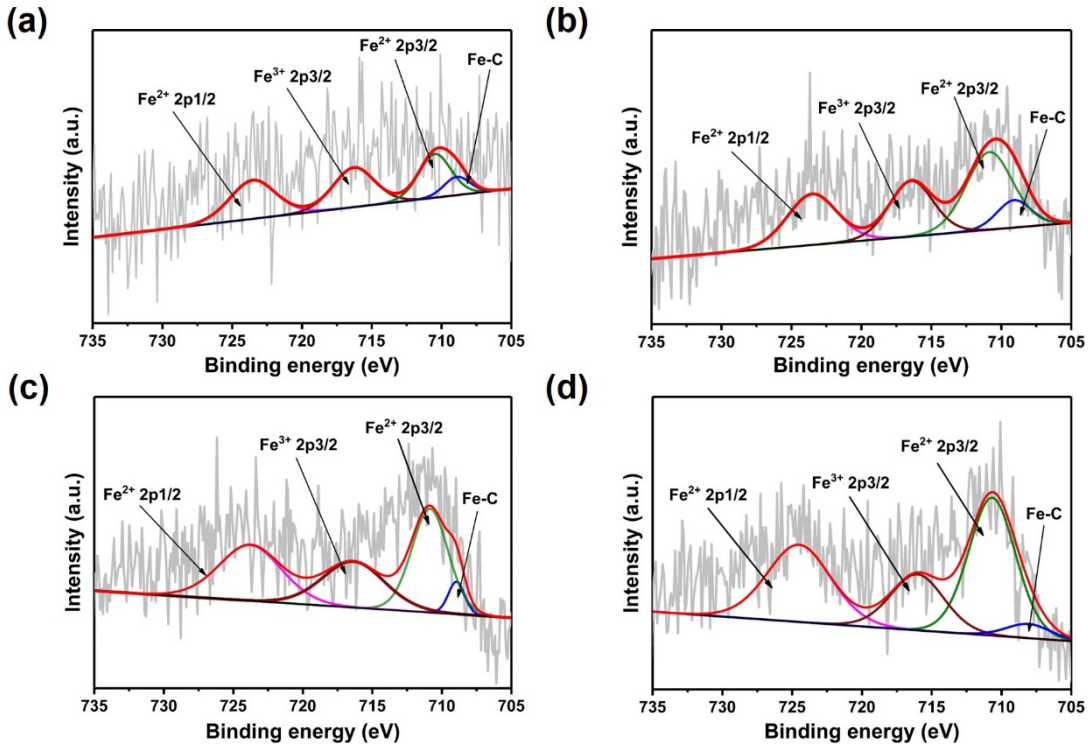

Fig. S6. Fe 2p XPS spectra of (a) Zn/Fe-NC-0.1, (b) Zn/Fe-NC-0.3, (c) Zn/Fe-NC-0.7 and (d) Zn/Fe-NC-0.9.

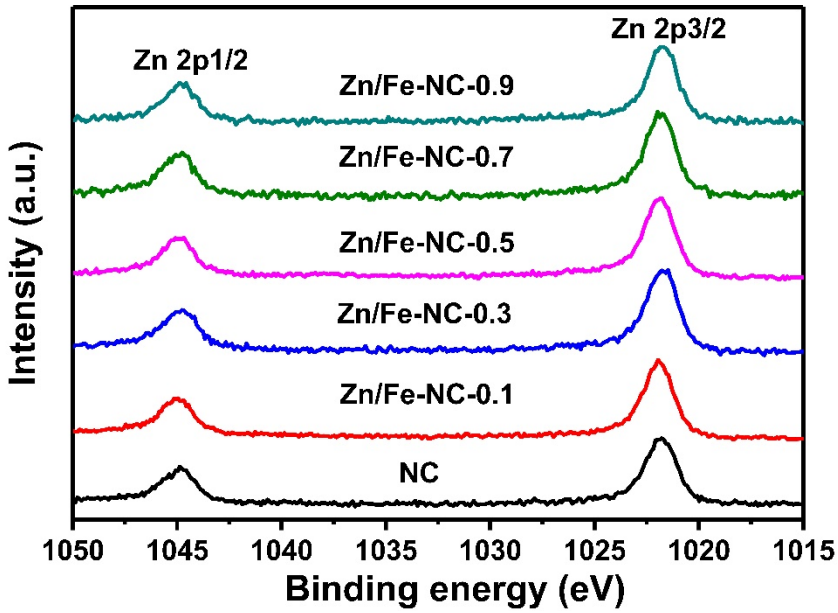

Fig. S7. Zn 2p XPS spectra of NC and Zn/Fe-NC-x.

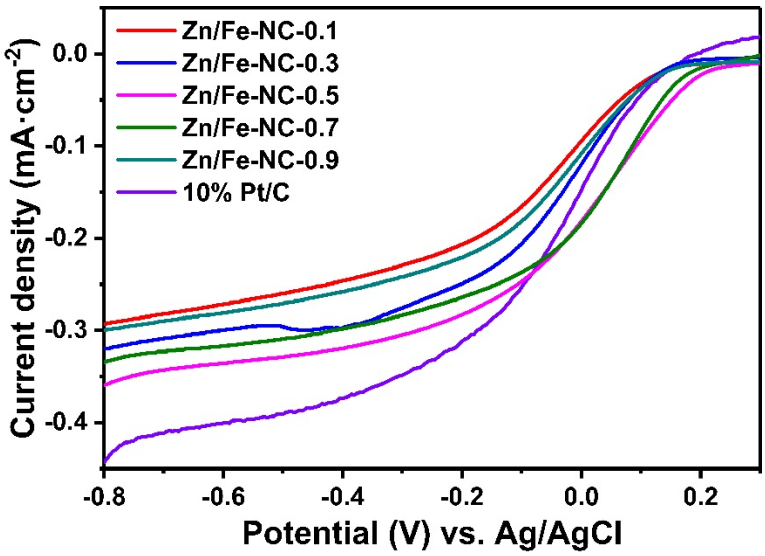

Fig. S8. LSV curves of different catalysts at a rotation rate of 1600 rpm.

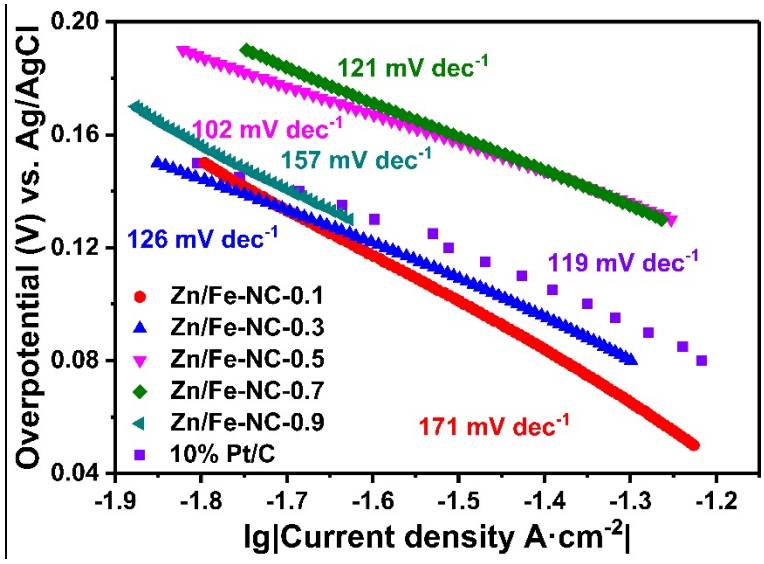

Fig. S9. Tafel curves of different catalysts at a rotation rate of 1600 rpm.

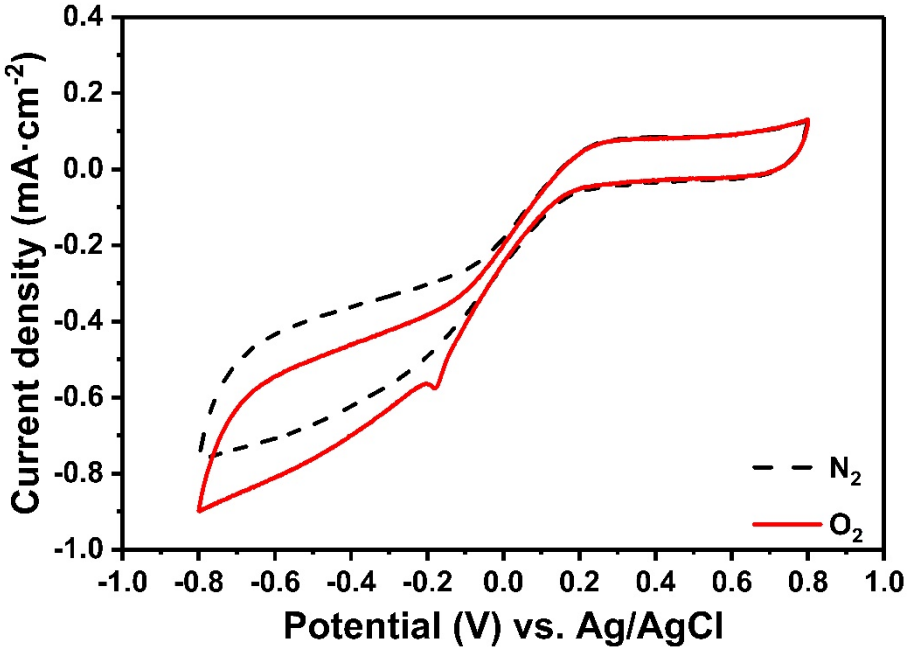

Fig. S10. CV curves of Zn/Fe-NC-0.5 at a rotation rate of 1600 rpm in O_2-saturated and N_2-saturated PBS solution.

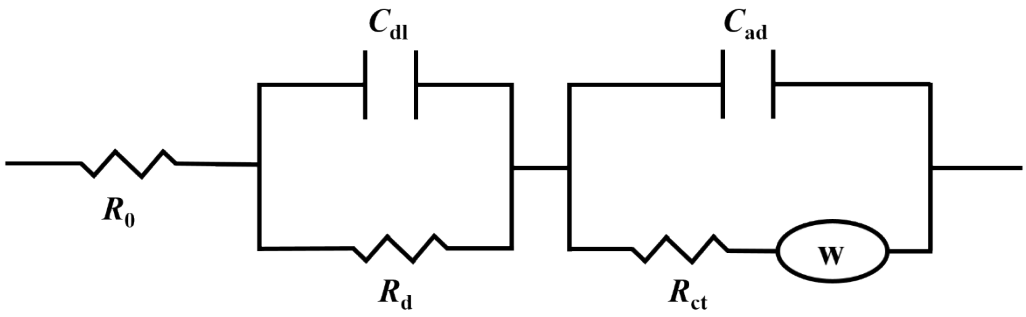

Fig. S11. Equivalent circuit of EIS modeling.

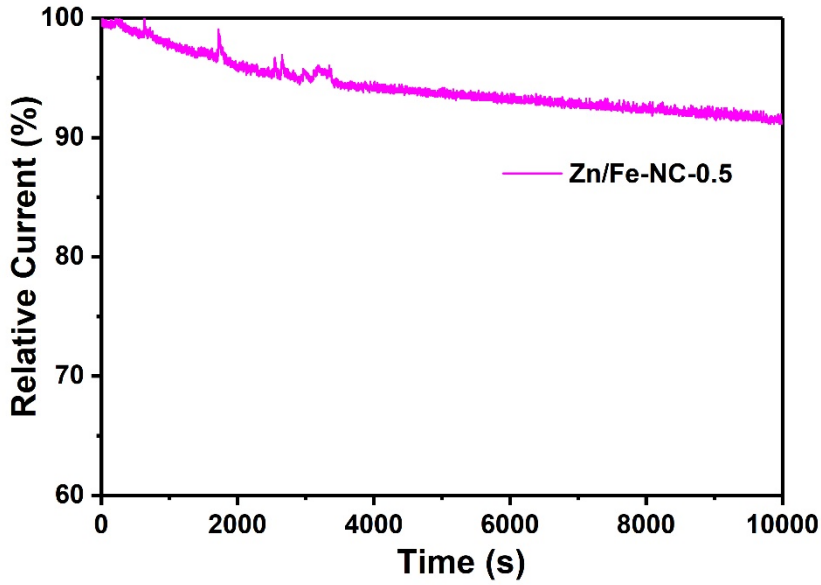

Fig. S12. I-t curve of Zn/Fe-NC-0.5 with the rotation speed of 1600 rpm.

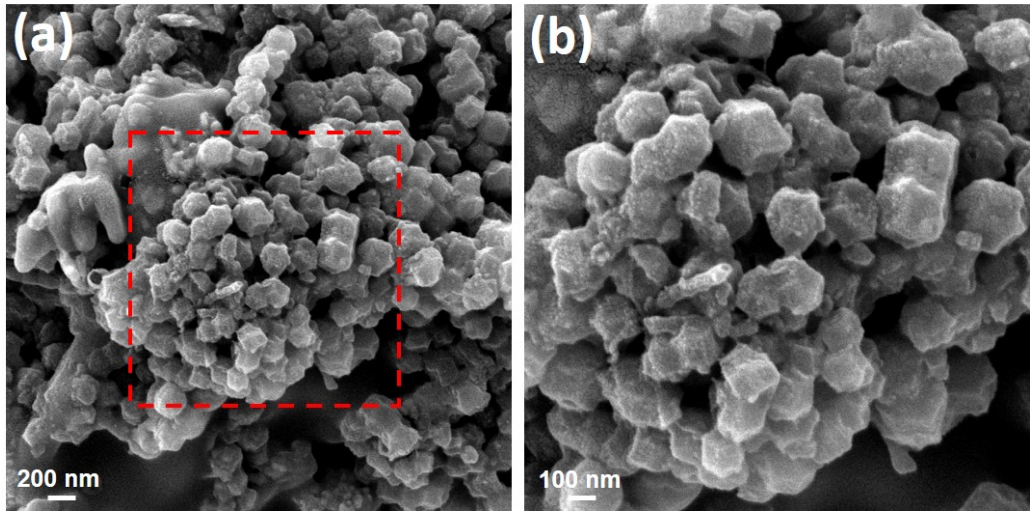

Fig. S13. SEM images after i-t test for 10000 s.

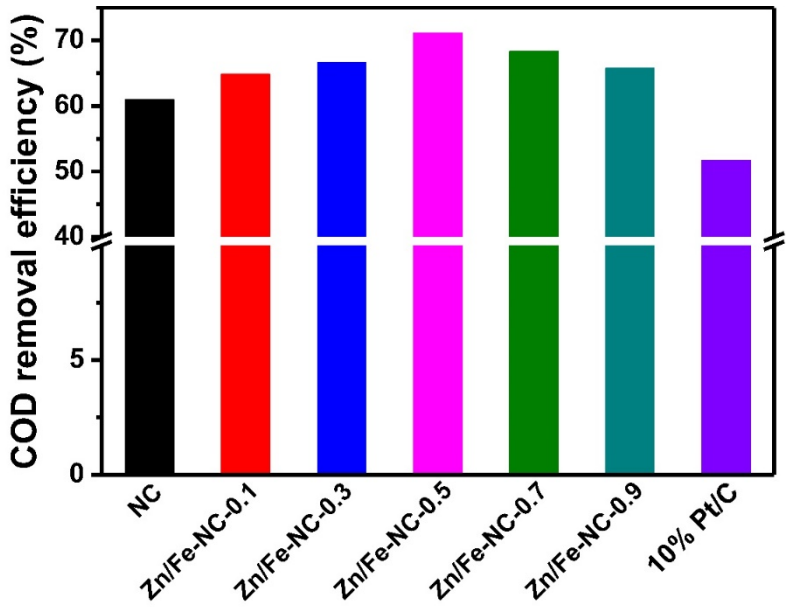

Fig. S14. COD removal efficiency of MFCs**.**

References

1. G. X. Yang, Z. Z. Zhang, X. H. Kang, L. H. Li, Y. Li and Y. M. Sun, *ACS Appl. Energy Mater.*, 2020, **3**, 11929-11938.
2. X. Luo, W. L. Han, W. C. Du, Z. M. Huang, Y. Jiang and Y. Zhang, *J. Power Sources*, 2020, **469**.
3. G. Lu, Y. Zhu, L. Lu, K. Xu, H. Wang, Y. Jin, Z. J. Ren, Z. Liu and W. Zhang, *J. Power Sources*, 2016, **315**, 302-307.
4. L. Zhou, C. Yang, J. Wen, P. Fu, Y. Zhang, J. Sun, H. Wang and Y. Yuan, *J. Mater. Chem. A*, 2017, **5**, 19343-19350.
5. C. Cao, L. L. Wei, G. Wang, J. T. Liu, Q. R. Zhai and J. Q. Shen, *Inorg. Chem. Front.*, 2017, **4**, 1930-1938.
6. M. Zhong, C. Ren, D. Z. Fang, C. C. Lv and K. X. Li, *J. Electroanal. Chem.*, 2020, **878**.